Towed array beamforming during ship's maneuvering

Paulo Felisberto **Sérgio M. Jesus**

November 3, 2001

Abstract. Towed hydrophone arrays are commonly used for determining the spatial characteristics of the underwater acoustic field. The assumption that the hydrophones lie in a straight and horizontal line is often made when beamforming the hydrophone outputs. However, due to tow vessel motion, ocean swells and currents the array adopts a nonlinear shape and the beamformer output is degraded. To estimate the positions of the hydrophones, an array was instrumented with a set of positioning sensors: compasses, tiltmeters, accelerometers and pressure gauges. This paper presents the array deformations recorded at sea when the tow vessel is turning and along straight line tracks. The influence of the observed deformations on the performance of the conventional beamformer output is discussed and ilustrated with simulated and real acoustic data.

1 Introduction

Towed arrays are widely used in underwater acoustics for estimating the horizontal directionality of the acoustic field. Fast plane-wave beamforming algorithms require the assumption that the array is straight and horizontal. The underlying justification is that the use of an equispaced and straight line array allows to important algorithmic simplifications leading to a dramatic increase of computing efficiency. Unfortunately, this assumption is not always fully verified in practice. In fact due to tow ship speed and course fluctuations, underwater currents, swell and other effects the array shape is often far from linear. It is faithful that the deviations from the linear shape are also dependent on the array construction parameters like lenght, thickness, number of mechanical sections and him liaisons. When the array deviates from the assumed linear shape, the beamformer output performance is degraded with bearing estimation errors, loss of beam power and increased side lobe levels. However, this problem can be avoided if the hydrophone positions can be estimated and the respective corrections introduced in the beamformer. Generally, two type of methods were used to estimate the acoustic sensor positions on a pertubed array. In the first type of methods, the array is instrumented with positioning

sensors like compasses, tiltmeters, pressure gauges and then some interpolation scheme is used to determine the hydrophone positions [1]. The second kind of methods are known as "data-driven", since they estimate the hydrophone positions from the acoustic data itself. These methods do not need any additional positioning sensors mounted on the array, but array shape estimation is, in this case, highly time consuming and in some cases sources at known far-field locations are needed [2]- [7].

In this paper we estimate hydrophone array deformations based on the information recorded at sea with a 156 m length array instrumented with several positioning modules. The non-acoustic data and the interpolation scheme used to estimate the hydrophone positions will be presented. Beamformer outputs are compared in different tow ship's maneuvering situations to analyze the influence of the array deviations from linearity. This work also addresses the problem of estimating the acoustic field directionality in the full 0-360 degrees range.

2 Beamforming of a deformed towed array

Beamforming is a well-known technique to observe the directionality of the acoustic field sampled by an hydrophone array. To observe signals from a given direction, the beamformer coherently adds the hydrophone outputs by adjusting their relative delays for that direction.

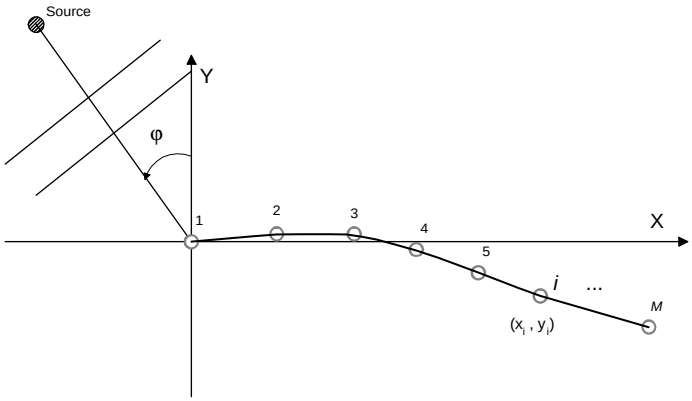

Figure 1: array axis system orientation

Frequently, beamforming is performed in the frequency domain, in which case the relative delays are replaced by the equivalent phases. Consider a plane-wave impinging at bearing ϕ on a towed array with M hydrophones uniformly spaced at d meters as shown in figure 1. Our interested will concentrate in the azimuthal bearing thus, only the deformations in the XY-plane will be considered. In the frequency domain the beamforming operation for a given l frequency bin can be written as [3]

$$G_{l,\phi} = \sum_{m=0}^{M-1} X_{l,m} \exp -j\frac{\omega_l}{c}\{x_m \sin\phi - y_m \cos\phi\} \tag{1}$$

where $X_{l,m}$ denotes the ω_l frequency component of the observation at hydrophone l, c is the sound speed, M is the number of sensors and (x_m, y_m) is m-th hydrophone position. Source bearing is estimated by finding the value of ϕ that maximizes (1). Generally, an implementation of (1) is very computational intensive, but it can be enhanced if the assumption that $x_m = m.d$ is made (i.e. we assume that the disturbance along the x-axis can be neglected). Defining the normalized spatial frequency (or wavenumber) k as

$$k = -\frac{\omega_l dM}{c2\pi}\sin\phi \quad -\pi/2 < \phi \leq \pi/2 \tag{2}$$

Thus, rewriting G as function of wavenumber k and using the approximation $x_m = m.d$

$$G^P_{l,k} = \sum_{m=0}^{M-1} X_{l,m} \exp -j\left\{\frac{km2\pi}{M}\right\} \exp -j\left\{y_m\sqrt{\left(\frac{\omega_l}{c}\right)^2 - \left(\frac{k2\pi}{dM}\right)^2}\right\} \qquad y \geq 0 \tag{3}$$

$$G^N_{l,k} = \sum_{m=0}^{M-1} X_{l,m} \exp -j\left\{\frac{km2\pi}{M}\right\} \exp +j\left\{y_m\sqrt{\left(\frac{\omega_l}{c}\right)^2 - \left(\frac{k2\pi}{dM}\right)^2}\right\} \qquad y \leq 0 \tag{4}$$

These expressions can be implemented more efficiently than (1), if some symmetries and similarities are explored. From this point of view, the most favourable case occurs when the array is straight and horizontal (all $y_m = 0$) in which case an FFT based algorithm can be applied. In order to have an idea of the quality of the approximation, a comparative study between the outputs from the approximated method (3)-(4) and the generalized method (1) has been made. This study showed that the approximated beampattern could not be distinguished from the true beampattern for sources at or near broadside and showed a maximum error of 5 dB for sources at or near endfire. That behaviour is approximately constant for any frequency below the maximum array working frequency.

A well-known drawback of the straight line array assumption is the left-right ambiguity. This ambiguity arises because the relative delays between sensors for a choosen source bearing are the same regardless of the source's left-right position. When the array is deformed this no longer happens and therefore the ambiguity problem can be solved. Analyzing G^P and G^N, we observe that the joinning maximum occurs in G^P if the source is in the right side of the array. The opposite happens for G^N that peaks for a source in the left side of the array.

3 Estimating the array deformation

A sketch of the array used in the experiment is depicted in figure 2. The array has 40 uniformly spaced hydrophones at 4m, placed in 3 acoustic mechanical sections and a tail element. To determine the hydrophone positions, the array was instrumented with the following set of positioning sensors:

- 6 compasses (C1 to C6);
- 6 tiltmeters (T1 to T6);
- 6 accelerometers (A1 to A6);
- 2 pressure gauges.

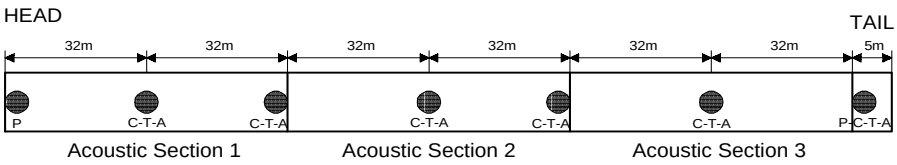

Figure 2: towed array configuration and positioning modules: C=compasses, T=tiltmeters, A=accelerometers and P=pressure gauges.

The pressure gauges were installed one in the array head and the other in the array tail. The compass C1, the tiltmeter T1 and the accelerometer A1, that form the first positioning module, were installed nearby the hydrophone closest to the ship (# 1). That hydrophone was choosen as the origin of the Cartesian positioning system. In this system, it is assumed that the x axis and the first compass direction are colinear. The absolute angles measured by the others compasses (C2 to C6) are transformed in relative angles to the x-axis by subtracting the values from compass C1. The positioning modules (each composed of one compass, one tiltmeter and one accelerometer) were placed at 32m intervals. To estimate the hydrophone's positions in between two adjacent modules a linear interpolation scheme with a 0.5 m griding was used. Consider the vector $(c_1, c_2, \ldots, c_N)$ as the interpolated compass values and the vector $(t_1, t_2, \ldots, c_N)$ as the interpolated tiltmeter values - N is the number of interpolation samples. To estimate the three dimensional coordinates $x_i, y_i, z_i; i = 1, \ldots, N$, the following expressions were used

$$\begin{aligned} x_i &= x_{i-1} + \delta \cos\phi_i \cos\lambda_i, \\ y_i &= y_{i-1} + \delta \cos\phi_i \sin\lambda_i, \\ z_i &= z_{i-1} + \delta \sin\phi_i, \end{aligned} \tag{5}$$

where $x_1 = 0$, $y_1 = 0$, $z_1 = 0$, $\delta = 0.5$ m is the interpolation interval and the angles were computed using

$$\begin{aligned} \phi_i &= -\frac{(t_i + t_{i-1})}{2}, \\ \lambda_i &= -\frac{(c_i + c_{i-1})}{2}. \end{aligned} \tag{6}$$

The hydrophone positions are a subset of the computed values for $i = 1, 9, 17, 25, \ldots$. This is a very simple procedure, that can be easily implemented in a "real-time" system with inexpensive hardware. Note that the z-coordinate is estimated here, but for our purposes, only the x and y coordinates were used when computing the beamformer output as described in section 2. Also, if the absolute depth is needed then these algorithms can be combined with the measurements obtained from the array head and tail pressure gauges. Initially, the installation of accelerometers was decided based on the observation that accelarations might be necessary to correct tiltmeter outputs since tiltmeters act like pendulums and therefore they are very sensitive to accelerations. During the cruise strong bias were observed on the accelerometer data and no correction seemed to be necessary on the tiltmeter outputs. In the sequel we will concentrate on the compass-tiltmeter data.

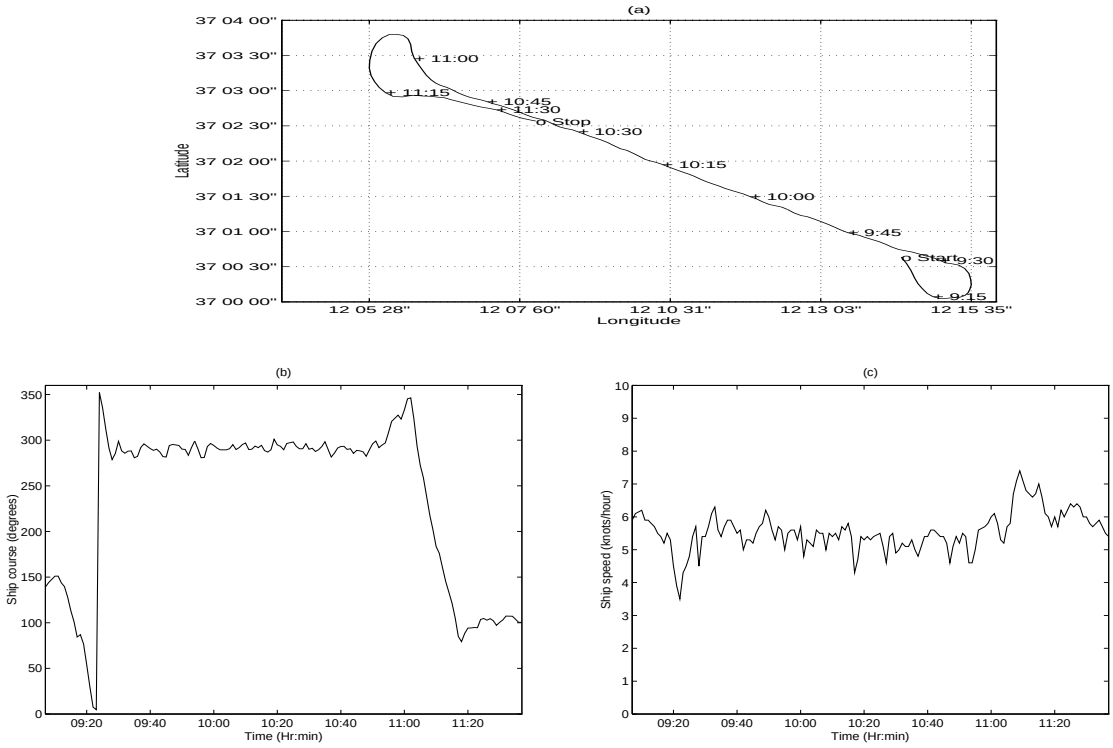

Figure 3: Ship navigation data during sea trial day 04 March 1994. Ship track in (a), ship course in (b) and ship ground speed in (c).

4 At sea data acquisition and processing

4.1 Tow vessel navigation data

The sea trial took place in the Strait of Sicily in the Pantelleria area. Figure 3 gives a general view of the tow vessel navigation data during day 04 of March of 1994. The ship made two 180 degrees port turns. At these moments, we expect significant disturbances in the array shape. Another, navigation parameter that is important in the array deformation is the ship's speed. As it can be seen ship's speed fluctuations are relatively small during straight-line tracks and only during the turns showed some variability.

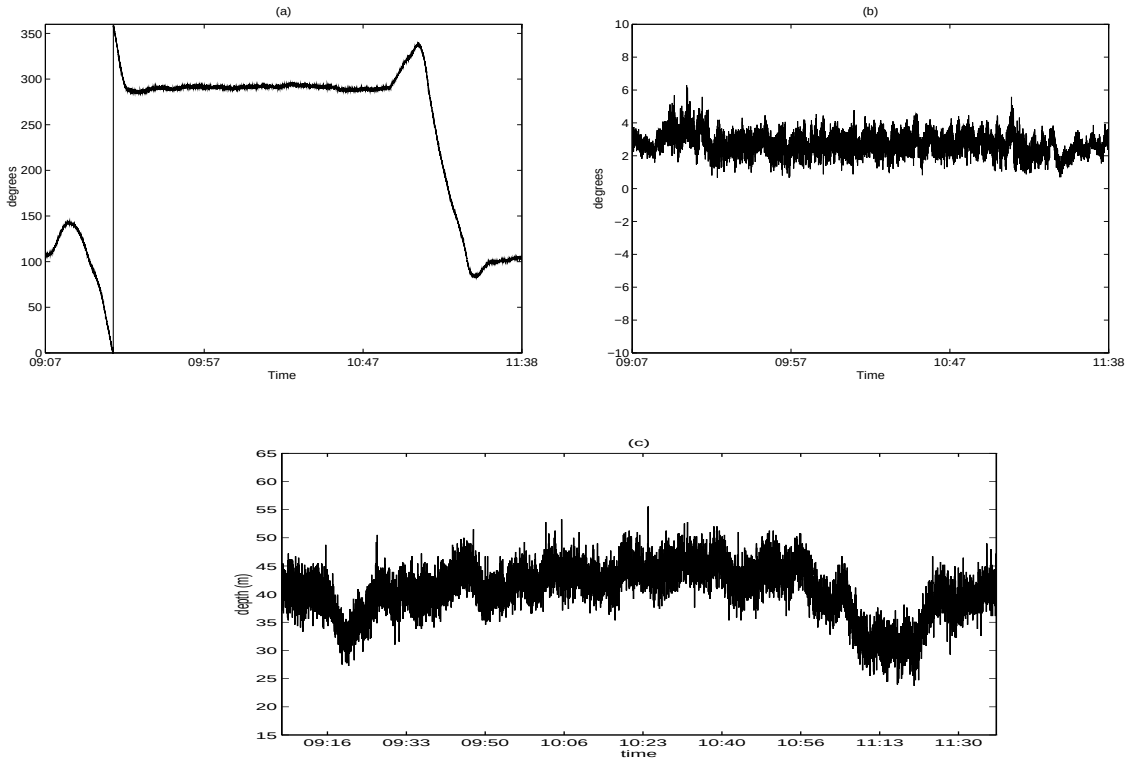

Figure 4: positioning data - compass(a), tiltmeter (b), pressure gauge(c)

4.2 Array positioning data

The positioning sensor data was acquired with a sampling rate of one sample per second. Output examples of positioning sensor data for the time interval 09:07 to 11:38 are presented in figure 4. Figure 4(a) shows the output data for one compass (a). The compasses diagrams are delayed replicas of the ship's course plot (figure 3(b)).

Data from one of the tiltmeters is shown in figure 4(b). This data needed to be filtered to eliminate the high

frequency components that are possibly due to flow noise. Also, from this plot the moments where the tow vessel turns are perceivable. Figure 4(c) presents data from the pressure gauge located in array head, after conversion to depth. From this curve, one can easily perceive when ship is turning. The output data from the other pressure gauge (located in array tail) has a similar evolution with a "constant" bias (about 10m), even during the turns.

4.3 Estimated array deformation from recorded positioning data

The array deformation was estimated using the procedure proposed in section 3. Figure 5 ilustrates a set of representative array shapes recorded before the turn (doted line), during the turn (dashdot line) and after the turn (dashed line).

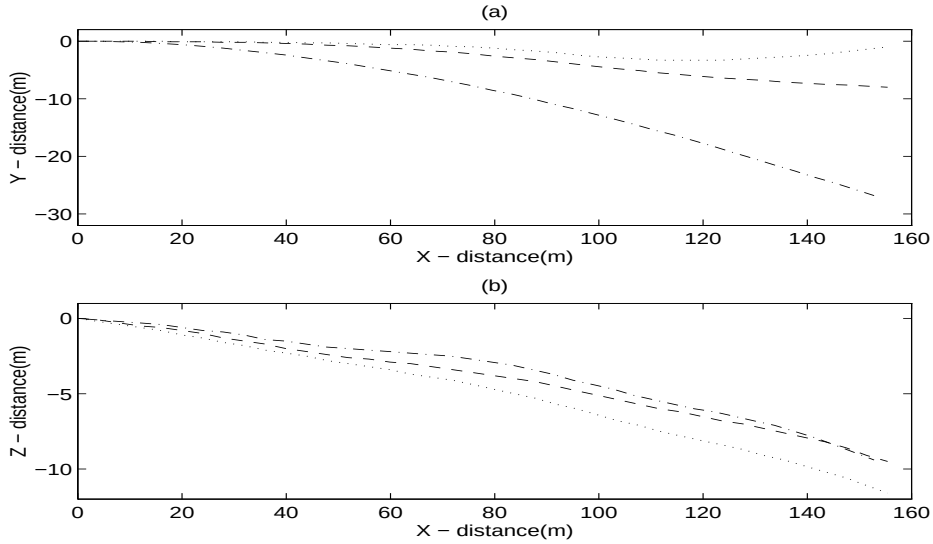

Figure 5: estimated array deformations before ship turn(...), during the turn (-.-) and after the turn (- - -) in the horizontal XY plane in (a) and in the vertical XZ plane in (b).

The spatial filtering characteristics of an array are sometimes ilustrated by the beam power pattern. In figure 6 its plotted the normalized beam power patterns according to the array deformations of figure 5 for the maximum work frequency of the array (187.5Hz) without steering. We remark that depending on the level of array deformation the beam power pattern for the portion of the plane complementary to the source has a lower main lobe but a larger beam width - something like a shade. This is the starting point to solve the right-left ambiguity problem. From these figures a difference up to 8 dB between the main lobe and the shade can be remarked. It can be shown that for the considered array and its observed deformations this difference generally increases with the array deformation, and the greater values are observed when the source is broadside to the

array and its frequency is close to the array maximum working frequency. Since plots in figure 6 represent the theoretical beam power patterns for the considered deformations, it is expected that in "real world" due to sensor errors, their related array shape estimation errors and other errors, the difference between the main lobe and the shade is somehow smaller than the theorectical.

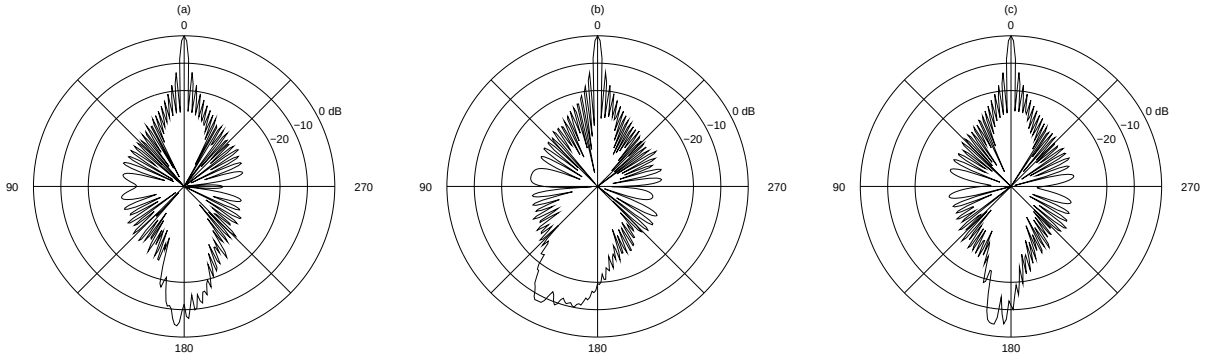

Figure 6: beam patterns for a broadside source with real array deformations according to figure 6 before ship turn (a), during the turn (b) and after the turn (c).

4.4 Processing the acoustic data

In this section real acoustic data has been processed with the beamforming expressions (3) and (4), which are approximations of (1). As an example of application to field data a few observations recorded at one minute interval during the second ship turn, between 11:05 and 11:08 am are presented in figures 7 to 10. The sampling frequency was 750 Hz and the block size used for FFT computation was equal to 1024 samples. No averaging was done and the number of beams was equal to 128. During that experiment, the ship was simultaneously towing a towed array and an acoustic source emitting tones at 100, 120 and 125 Hz. The acoustic field is essentially composed by the towed source signal at bearing 90 degrees and a strong nearby merchant ship echo, covering the frequency range from 60 up to 180 Hz, close to broadside. There is a number of other minor noise sources possibly due to distant ships close to endfire. The sequence of observed array deformations are ilustrated in figures 7(a) to 10(a). One can remark that the array deformation is progressively increasing on the XY plane up to 38 m deviation at the array tail relative to the first hydrophone. Along this sequence, figures 7(b) to 10(b), show the beamformer output assuming a straight line array. Figures 7(c) to 10(c), present the beamformer output using expressions (3) and (4) with the estimated array deformations shown in figures 7(a) to 10(a) respectively. In the 360 degrees plots, frequency increases linearly from 0 Hz in the center to 187.5 Hz

(the maximum working frequency) in the border.

Figure 7, with an almost straight line array, the strong ship echo at 10 degrees can be clearly seen together with the three towed source tones. The 360 degrees plot, figure 7(c), shows that the left-right ambiguity can not be resolved. Figures 8 to 10, with a progressive array deformation, show that the strong ship echo is being smeared on plot (b) (that assumes a straight line array) and the towed source tones can not be distinguished from background noise. Simultaneously, the 360 degrees plots show an increasing difference on the acoustic field received from the left and right sides of the array. A close analysis of this difference confirms that the strong ship echo is effectively located starboard at 10, 0, -10 and -45 degrees from figure 7(c) to 10(c) respectively.

5 Conclusions

This paper has shown a number of non-acoustic measurements aimed at estimating towed array deformations at sea. According to these observations it can be concluded that a towed array is never straight nor horizontal. As expected, this deviation from linearity is higher when the ship turns. In this case the beamformer output is highly reduced, inducing bearing estimation errors, loss of beam power and increased side-lobe levels. This paper presents a simple and fast method to estimate the array deformation based on the non-acoustic positioning data recorded on real-time and to include these deformation into the beamformer. It is shown that, depending on the deformation of the array, the left-right ambiguity can be resolved. The proposed models to estimate the array shape and the acoustic field directionality were successfully applied on real data where right and left sources could be unambigously located on a 0-360 degrees ring.

Acknowledgments

The authors wish to acknowledge A. Kristiansen and A. Caiti, Scientists in Charge, the master and crew of the R/V ALLIANCE and the SACLANT Centre Enginnering Department for their outstanding respective contributions in the leadership, sea-going operation and equipment preparation before and during the sea trial. The support of E. Dias and E. Coelho from the Hydrographic Institute, Lisbon, on the acquisition of the non-acoustic data is also appreciated. This work was supported by the Marine Science and Technology (MAST II) programme of EEC under contract MAS2-CT920022.

References

[1] Bernard E. Howard and James M. Syck, "Calculation of the shape of towed underwater acoustic array", *IEEE Journal of Oceanic Engineering*, 1992, vol. 17, pp. 193-203.

[2] Homer P. Bucker, "Beamforming a towed line array of unknown shape", *Journal of Acoustical Society of America*, 1978, vol. 63, pp. 1451-1454.

[3] Daniel E. Wahl, "Towed array shape estimation using frequency wavenumber data", *IEEE Journal of Oceanic Engineering*, 1993, vol. 18, pp. 582-590.

[4] Michel Bouvet, "Beamforming of a distorted line array in the presence of uncertainties on the sensor positions", *Journal of Acoustical Society of America*, 1987, vol. 81, pp. 1833-1840.

[5] Brian G. Ferguson, "Sharpness applied to the adaptive beamforming of acoustic data", *Journal of Acoustical Society of America*, 1990, vol. 88, pp. 2695-2701.

[6] Barry G. Quinn, Ross F. Barrett, Peter J. Kootsookos and Stephen J. Searle, "The estimation of the shape of an array using a hidden Markov model", *IEEE Journal of Oceanic Engineering*, 1993, vol. 18, pp. 557-564.

[7] Brian G. Ferguson, "Remedying the effects of array shape distortion on the spatial filtering of acoustic data from a line array of hydrophones", *IEEE Journal of Oceanic Engineering*, 1993, vol. 18, pp. 565-571.

[8] Shi-Wei Gao and J. W. R. Griffiths, "Experimental performance of high-resolution array processing algorithms in a towed sonar array environment", *Journal of Acoustical Society of America*, 1994, vol. 95, pp. 2068-2080.

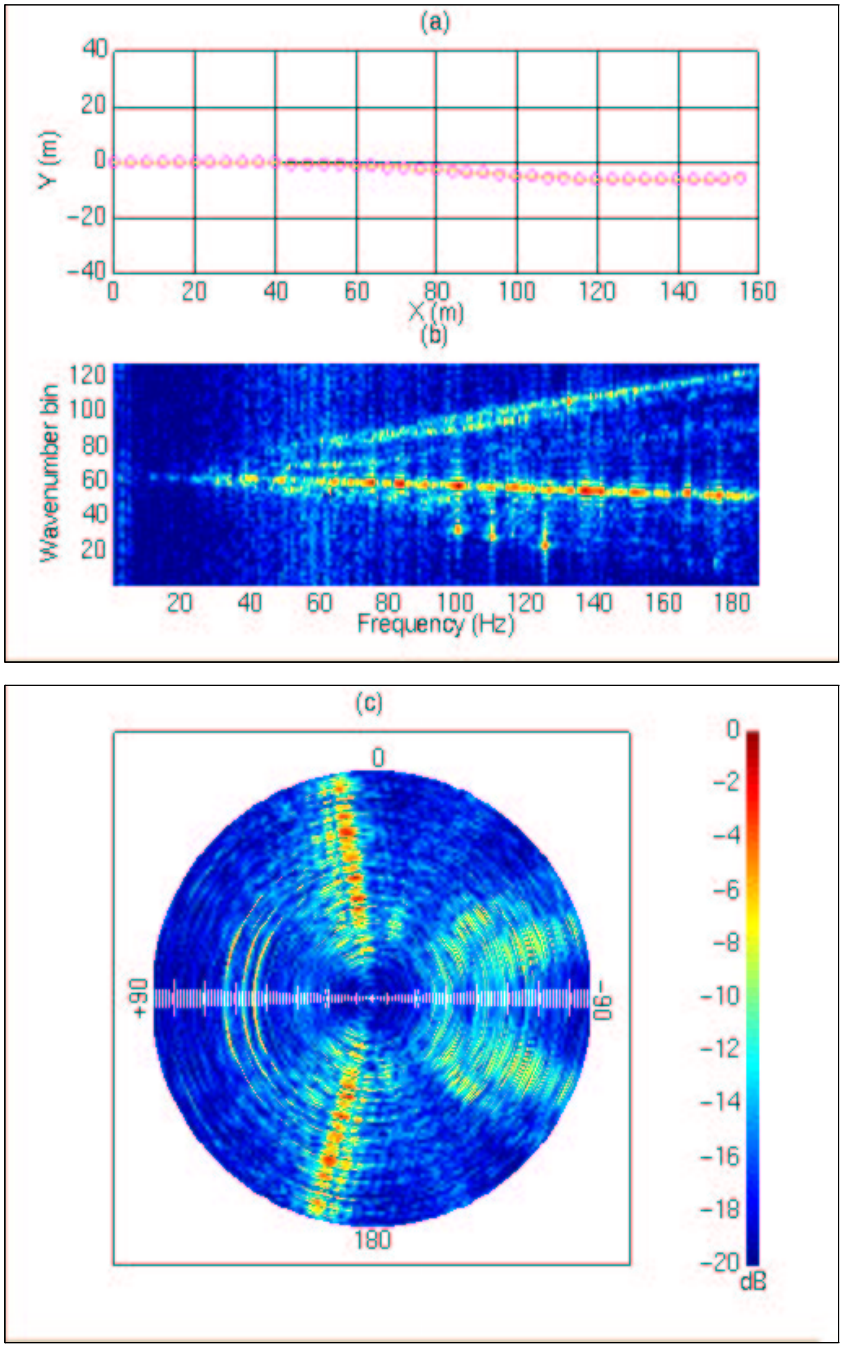

Figure 7: field towed array data at 11:05 am: XY plane array deformation (a), beamformer output assuming a straight line array (b) and beamformer output spanning 360 degrees considering the array deformation of (a)-frequency increases from centre (0 Hz) to border (187.5 Hz) (c).

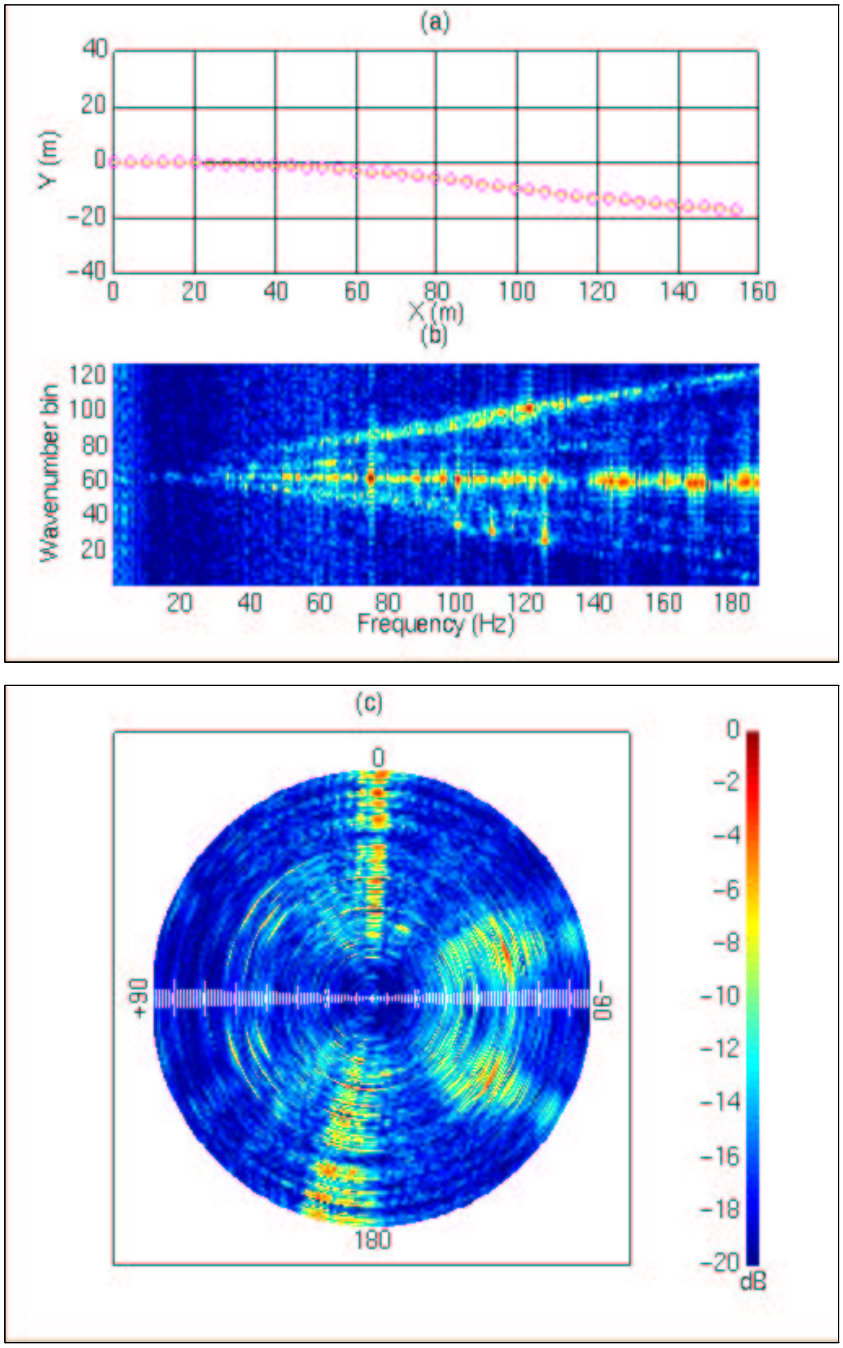

Figure 8: field towed array data at 11:06 am: XY plane array deformation (a), beamformer output assuming a straight line array (b) and beamformer output spanning 360 degrees considering the array deformation of (a) - frequency increases from centre (0 Hz) to border (187.5 Hz) (c).

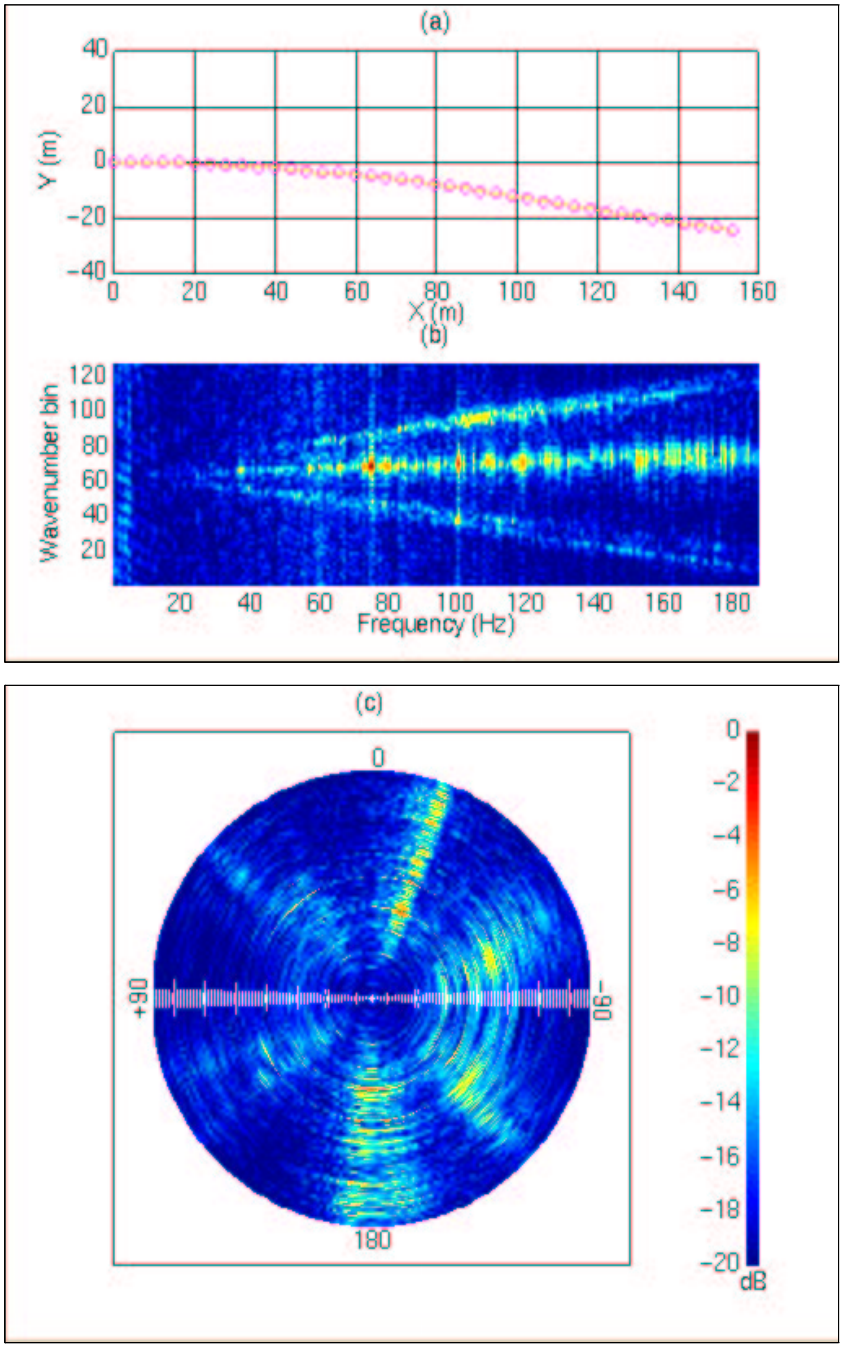

Figure 9: field towed array data at 11:07 am: XY plane array deformation (a), beamformer output assuming a straight line array (b) and beamformer output spanning 360 degrees considering the array deformation of (a) - frequency increases from centre (0 Hz) to border (187.5 Hz) (c).

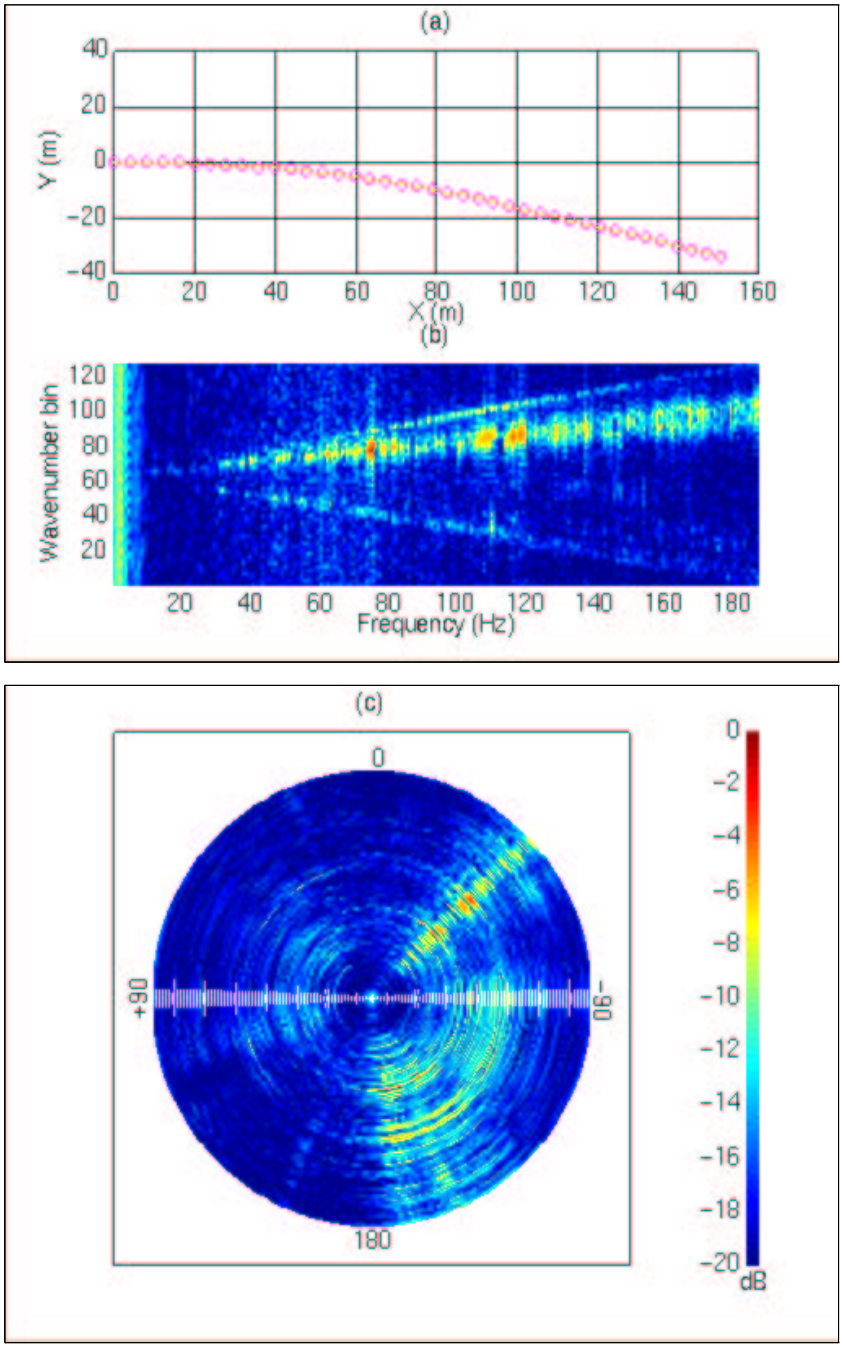

Figure 10: field towed array data at 11:08 am: XY plane array deformation (a), beamformer output assuming a straight line array (b) and beamformer output spanning 360 degrees considering the array deformation of (a) - frequency increases from centre (0 Hz) to border (187.5 Hz) (c).